

# *Estimation of Side Slip in Vehicles*

Dual Degree Project Dissertation

Submitted in partial fulfillment of the requirements  
for the award of Bachelors and Masters degree

in

Mechanical Engineering  
Computer Aided Design and Automation

by

**Jasvipul Singh Chawla**

**(01D10006)**

*Under the Guidance of*

**Prof. S. Suryanarayanan**



**DEPARTMENT OF MECHANICAL ENGINEERING  
INDIAN INSTITUTE OF TECHNOLOGY, BOMBAY**

**June 2006**

# *Abstract*

This work proposes a methodology to estimate tire side slip angles in front-wheel steered, rear-wheel driven four wheeled vehicles. A three degree-of-freedom model with slip angle, yaw rate and roll angle as degrees of freedom was constructed to capture the coupling between steering and roll dynamics of such vehicles. An open-loop estimator was designed based on this model to estimate the side slip angles of tires using available real-time measurements which include steering angle, steering torque and suspension positions. The estimator was validated by comparing its predictions with that of an ADAMS model. The predictions of the ADAMS model in turn were compared with experimental results reported in vehicle dynamics literature for similar vehicles and test conditions. We conclude that a three degree-of-freedom model is a good start for use in estimation techniques of side slip angle.

# Contents

<b>List of figures</b>	<b>v</b>
<b>Nomenclature</b>	<b>vi</b>
<b>1. Introduction</b>	<b>1</b>
1.1. Motivation and Objectives	1
1.2. Contribution of the Project	2
1.3. Organization of the Report	2
<b>2. Preliminaries</b>	<b>3</b>
2.1. Introduction	3
2.2. Dynamics of Vehicles	3
2.3. Steering and Suspension Mechanisms	4
2.3.1. Rack and Pinion Steering	4
2.3.2. Double Wishbone Suspension	4
2.3.3. Strut-McPherson Suspension	4
2.4. Coupling of Steering and Suspension Mechanisms	5
2.5. Lateral Force and Tire Slip Angle	6
2.6. Vehicle Models	6
2.6.1. Bicycle Model	6
2.6.2. Three Degree of Freedom Automobile Model	8
2.7. Observers	10
2.8. Current Approaches to Measure Side Slip	10
<b>3. ADAMS Model and Experimental Verification</b>	<b>13</b>
3.1. Introduction	13
3.2. Static Model	13
3.2.1. Model Assumptions	13
3.2.2. Model Predictions	14
3.3. Dynamic Model	15
3.3.1. Model Assumptions	15
3.3.2. Test Conditions	16
3.3.3. Model Predictions	17
3.4. Experiments of Test Vehicle	19
3.4.1. Data Acquisition	20
3.4.1.1. Vehicle Used	20
3.4.1.2. Hardware for Interfacing Sensors to Computer	20
3.4.1.3. Suspension Travel	20
3.4.1.4. Steering Torque and Angle	21

3.4.1.5. Yaw Rate and Lateral Acceleration	22
3.4.2. Summary of Estimation Methodology	22
3.4.3. Vehicle Tests	22
3.4.3.1. Constant Speed around Circle of Fixed Radius	22
3.4.3.2. Decreasing Speed around Circle of Fixed Radius	23
3.5. Observations	25
3.6. Discussion	26
<b>4. Conclusions and Future Work</b>	<b>27</b>
4.1. Conclusion	27
4.2. Future Work	27
<b>References</b>	<b>28</b>

# List of Figures

Figure 2.1 Vehicle Coordinate System	3
Figure 2.2: Rack and Pinion Steering Mechanism	4
Figure 2.3a: Double Wishbone Suspension	5
Figure 2.3b: Strut-McPherson Suspension	5
Figure 2.4: Coupled Suspension and Steering Mechanism	5
Figure 2.5: Lateral Force, Slip Angle	6
Figure 2.6: Bicycle Model	7
Figure 2.8: Three DOF Automobile Model	8
Figure 2.9: Observer Algorithm	10
Figure 3.1: ADAMS Static Model	14
Figure 3.2: Lateral Force vs. Steering Torque	15
Figure 3.3 ADAMS model of 3 DOF vehicle model	16
Figure 3.4 a: Steering Input for on-centre event (ADAMS Model)	18
Figure 3.4 b: Steering Force for on-center event (ADAMS Model)	18
Figure 3.5a: Yaw Rate for on-centre event (ADAMS Model)	18
Figure 3.5b: Front Tires' Slip Angles for on-centre (ADAMS Model)	18
Figure 3.6a: Roll Angle for on-centre event (ADAMS Model)	18
Figure 3.6b: Experimental Values from (4)	18
Figure 3.7a: Slip Angle vs. Lateral Acceleration (ADAMS)	19
Figure 3.7b: Experimental Values of Slip Angle vs. Lateral Acceleration from (8)	19
Figure 3.8a: Steering Angle vs. Lateral Acceleration (ADAMS Model)	19
Figure 3.8b: Experimental Values (8)	19
Figure 3.9: Arrangement of gears and potentiometer for measuring suspension travel	21
Figure 3.10: Experimental data and Side Slip Angle Estimates for Longitudinal Speed 20 kmph around 11m radius curve	23
Figure 3.11: Experimental data and Side Slip Angle Estimates for Decreasing Longitudinal Speed around 11m radius curve	24
Figure 3.12: Side Slip Angle Estimates from ADAMS model	25

# *Nomenclature*

X	Longitudinal Direction
Y	Lateral (Transverse Direction)
Z	Vertical Direction
F	Force
M	Moment
m	Mass
I	Moment of Inertia
$\alpha$	Tire Slip Angle
$C_{\alpha}, K$	Cornering Stiffness
u, V	Velocity
r,	Yaw Rate
$\beta$	Vehicle Slip Angle
$\delta$	Steer Angle
$\phi$	Roll Angle
$\psi$	Vehicle Yaw Angle
$\gamma$	Direction of Velocity
l	Distance from Centre of Gravity

## **Subscripts:**

x	longitudinal
y	lateral
z	vertical
f	of the front
r	of the rear
s	sprung
$\phi$	of roll

## **Abbreviations:**

DOF	Degree of Freedom
CG	Centre of Gravity
SUV	Sports Utility Vehicle
ADC	Analog to Digital Converter

# *Chapter 1*

## ***Introduction***

### *1.1 Motivation and Objectives*

The focus of the project is to estimate side slip angle in front-wheel steered, rear-wheel driven four wheeled vehicles in real time. Side slip angle gives a measure of the lateral forces produced at the tire-road contact patches while cornering which make the vehicle turn. Physically it represents the twist in the treads of the tires.

It is very difficult if not possible to directly measure the side slip angles of the tires, hence indirect methods have to be applied to estimate them. Knowledge of side slip angle is a required for advanced vehicle control systems like braking control, stability control, security actuators and for validating vehicle simulators. These controllers increase the safety of the vehicle, and make the response more predictable. The knowledge of slip angle can also be applied to decrease road damage caused by vehicles.

The wheel hub is coupled to the vehicle through the suspension and steering mechanisms. Thus the steering and suspension mechanisms affect each other's behavior. While cornering, changes will be induced in variables associated with both the mechanisms. The project endeavors to analyze these changes to estimate side slip angle based on suspension deflection information. This work has been performed to meet the following objectives:

1. To develop a method of estimating side slip angle in front-wheel steered four wheel vehicles.
2. To instrument a vehicle and conduct on road tests to validate the estimation method.

A model is constructed in ADAMS to simulate test conditions and predict the side slip angles for the tests to be conducted on the SUV. The predictions of this model are verified with experimental results from literature. An open-loop estimator that uses a

three degree-of-freedom vehicle model is used to estimate side slip angles using real time experimental data from tests conducted on an SUV. The estimates of side slip angles from on-road testing of the SUV using the open-loop estimator match with the predictions of the ADAMS model for quasi-static maneuvers. We conclude that a three degree-of-freedom model is a good start for use in estimation techniques of side slip angle.

## *1.2 Contribution of the Project*

*Contribution to Vehicle Manufacturers:* Using the methodology described in the project, side slip angle can be reasonably estimated in real-time using easily measurable variables. This can be adopted by vehicle manufacturers and put to use in high-end vehicles using advanced control systems.

*Contribution to Steer-By-Wire Project at IIT Bombay:* IIT Bombay is currently involved in making a Proof-of-Concept Steer-by-Wire project. Estimation of side slip angle will prove useful to enhance the performance of the associated controller.

## *1.3 Organization of the Report*

The report is divided into four chapters. The first chapter gives an introduction to the project and the objectives of the current study. The second chapter contains the relevant information about the architecture of the vehicle, mathematical models used and review about the commonly used techniques of side slip estimation. The third chapter explains the simulations and tests that have been conducted, and presents the results and discussions. Conclusions deduced from the current study and the suggestions for the future work have been summarized in the last chapter.

# Chapter 2

## Preliminaries

### 2.1 Introduction

This chapter gives the basic information required to understand vehicle architecture as well as dynamic behavior of front wheel steered, four wheel vehicles. It also explains how lateral forces are generated while a vehicle negotiates a turn, and their relation with the slip angle. Two vehicle models are discussed in detail. One of these models is used to build observers (estimators) for estimating side slip angle. A brief explanation of currently employed methods of estimation of side slip is given at the end of the chapter.

### 2.2 Dynamics of Vehicles

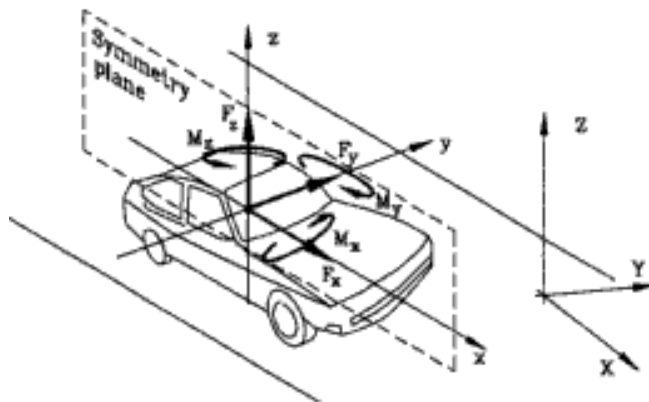


Figure 2.1 Vehicle Coordinate System

The vehicle coordinate system shown in the Figure 2.1 is explained below:

Linear motion along x dir is known as longitudinal motion.

Rotational motion about x axis is known as roll.

Linear motion along y dir is known as lateral or transverse motion.

Rotational motion about y axis is known as pitch.

Linear motion along z dir is known as vertical motion.

Rotational motion about z axis is known as yaw.

## 2.3 Steering and Suspension Mechanisms

### 2.3.1 Rack and Pinion Steering

The Rack and Pinion steering (Figure 2.2) is the most common steering mechanism for cars, SUVs and light trucks (1), (2). The driver gives input to the steering wheel which in turn rotates a pinion gear through steering shaft. The pinion is connected to a rack which moves laterally when the pinion rotates. Tie rods at each end of the rack move the tire spindle according to the movement of the rack. The tie rods are connected to the wheel hub and the rack through spherical joints which make the 4-bar a spatial mechanism. The dimensions of the bars are determined according to Ackerman Geometry considerations. (1).

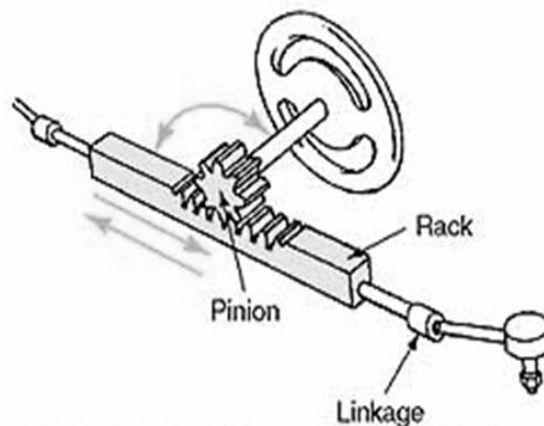


Figure 2.2: Rack and Pinion Steering Mechanism (2)

### 2.3.2 Double Wishbone Suspension

In a double wishbone suspension also known as Long Short Arm (LSA) suspension (Figure 2.3a), the wheel spindle is held between two wishbones or control arms by revolute joints to allow for steering motion (1). A damper and coil spring which acts as a shock absorber is attached between the lower control arm and the vehicle body.

### 2.3.3 Strut-McPherson Suspension

Strut-McPherson Suspension (Figure 2.3b) (1), (2) consists of a small sub frame (an A-arm) which provides a bottom mounting point for the hub or axle of the wheel. This

sub frame provides both lateral and longitudinal location of the wheel. The upper part of the hub is rigidly fixed to the inner part of the strut, the outer part of which extends upwards directly to a mounting in the body shell of the vehicle. The strut carries the coil spring on and a damper which acts as a shock absorber.

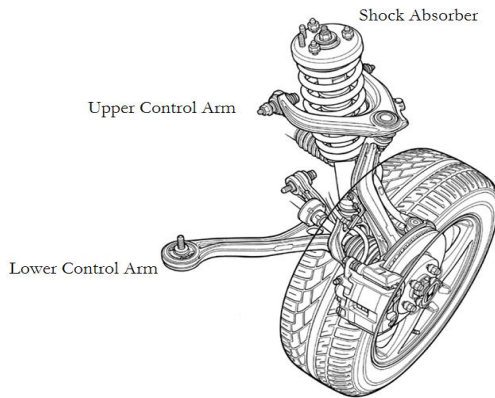


**Figure 2.3a: Double Wishbone Suspension (2)**

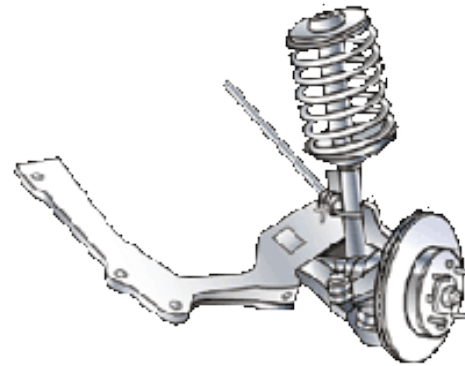


**Figure 2.3b: Strut-McPherson Suspension (2)**

## *2.4 Coupling of Steering and Suspension Mechanisms*

As the wheel hub is coupled to both the steering and suspension linkages through spherical joints, the combined system behaves like a 3-DOF 4-bar spatial mechanism. The orientation of the spatial mechanism depends upon steering input, and the left and right suspension travel (Figure 2.4). In vehicles using an anti-roll bar, some amount of force from left suspension is transferred to the right and vice-versa, by the anti-roll bar.



**Figure 2.4: Coupled Suspension and Steering Mechanism (2)**

## 2.5 Lateral Force and Tire Slip Angle

While cornering, a vehicle undergoes lateral acceleration, (3), (1). As the tires provide the only contact of the vehicle with the road, they must develop forces which result in this lateral acceleration. When a steering input is given, the successive treads of the tires that come in contact with the road are displaced laterally with respect to the treads already in contact with the road. Thus an angle is created between the angle of heading and the direction of travel of the tire. This angle is known as the tire slip angle which gives an estimate of twist of the treads of the tire. It can also be defined as the ratio of the lateral and forward velocities of the wheel. The twisted treads try to get back to their original positions, thus producing the force required for lateral acceleration (2) (Figure 2.5). This force is known as the Lateral Force ( $F_y$ ) or the Cornering Force. At a given load, the cornering force grows with slip angle. At low slip angles (5 degrees or less) the relationship is linear. In this region, cornering force is often described as  $F_y = C_\alpha \alpha$ . The proportionality constant  $C_\alpha$  is known as cornering stiffness and is defined as the slope of the curve for  $F_y$  versus  $\alpha$  at  $\alpha = 0$  (3).

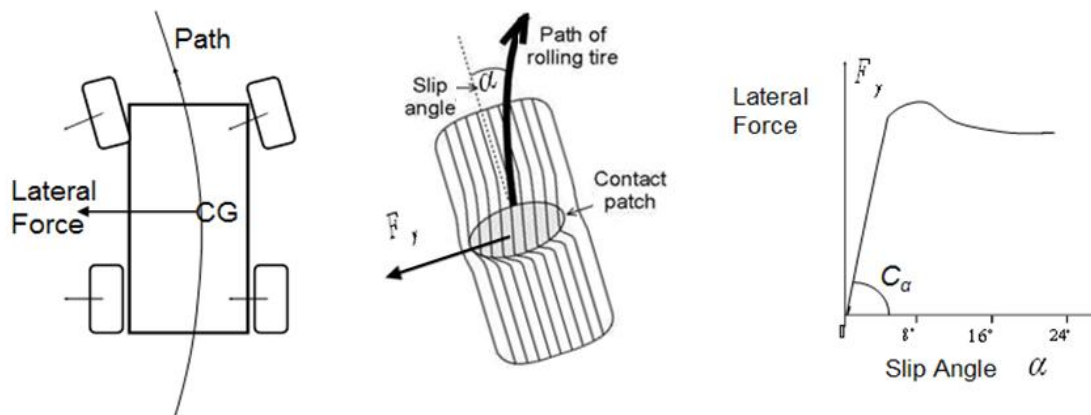


Figure 2.5: Lateral Force, Slip Angle (3)

## 2.6 Vehicle Models

### 2.6.1 Bicycle Model

The simplest model used to investigate lateral vehicle response is the linear two degree-of-freedom ‘bicycle model’ (4) (Figure 2.6). This model lumps the left and right tires at the front and rear of the car into equivalent tires located at the car center line, assuming that the slip angles on the inside and outside wheels are approximately the same. The degrees-of-freedom for constant forward speed are lateral velocity,  $u_y$  (or sideslip angle,  $\alpha$ ), and yaw rate,  $r$ . The steer and slip angles are assumed to be. Thus the tire forces may be assumed to vary linearly with slip angles. The longitudinal speed of travel is assumed to be constant. In addition, this model neglects body roll and load transfer.

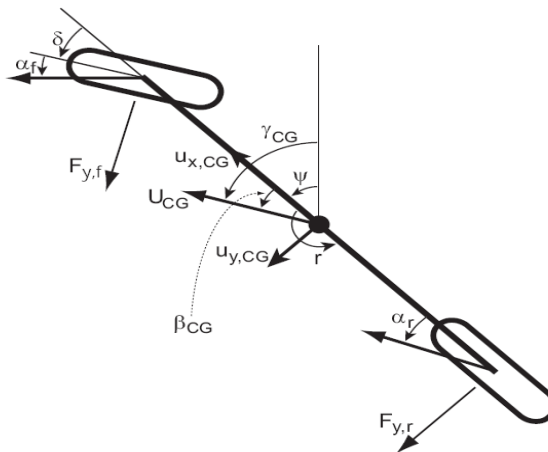


Figure 2.6: Bicycle Model (4)

In Figure 2.6,  $\delta$  is the steering angle,  $u_x$  and  $u_y$  are the longitudinal and lateral components of the vehicle velocity,  $F_{yf}$  and  $F_{yr}$  are the lateral tire forces, and  $\alpha_f$  and  $\alpha_r$  are the tire slip angles. The state equation for the bicycle model can be written as:

$$\begin{matrix} \dot{u}_{y,CG} \\ \dot{r} \end{matrix} = \begin{matrix} \frac{C_f}{m} & \frac{C_r}{m} \\ \frac{C_f a}{I_z} & \frac{C_r b}{I_z} \end{matrix} \begin{matrix} u_{x,CG} \\ u_{y,CG} \end{matrix} + \begin{matrix} \frac{C_r b}{m u_{x,CG}} & \frac{C_f a}{m} \\ \frac{C_f a^2}{I_z u_{x,CG}} & \frac{C_r b^2}{I_z u_{x,CG}} \end{matrix} \begin{matrix} r \\ r \end{matrix} \quad (2.1)$$

$I_z$  is the moment of inertia of the vehicle about its yaw axis,  $m$  is the vehicle mass,  $a$  and  $b$  are distance of the front and rear axles from the CG, and  $C_{\alpha f}$  and  $C_{\alpha r}$  are the total front and rear cornering stiffness. Given the longitudinal and lateral velocities,  $u_x$  and  $u_y$ , at any point on the vehicle body, the side slip angle can be defined by:

$$\tan^{-1} \frac{u_x}{u_y} \quad \text{---(2.2)}$$

The side slip angle at the center of gravity (CG) is shown by  $\beta_{CG}$  in Figure 2.6. The side slip angle can also be defined as the difference between the vehicle yaw angle ( $\psi$ ) and the direction of the velocity ( $\gamma$ ) at any point on the body.

$$\text{---(2.3)}$$

### 2.6.2 Three Degree of Freedom Automobile Model

Here, the vehicle is modeled with three degrees of freedom which include slip angle, yaw rate  $r$ , roll angle  $\phi$  (5). Note that this model takes into consideration the roll angle of the vehicle, which the conventional ‘bicycle model’ does not consider. The model is discussed below (Equations 2.4-2.11).

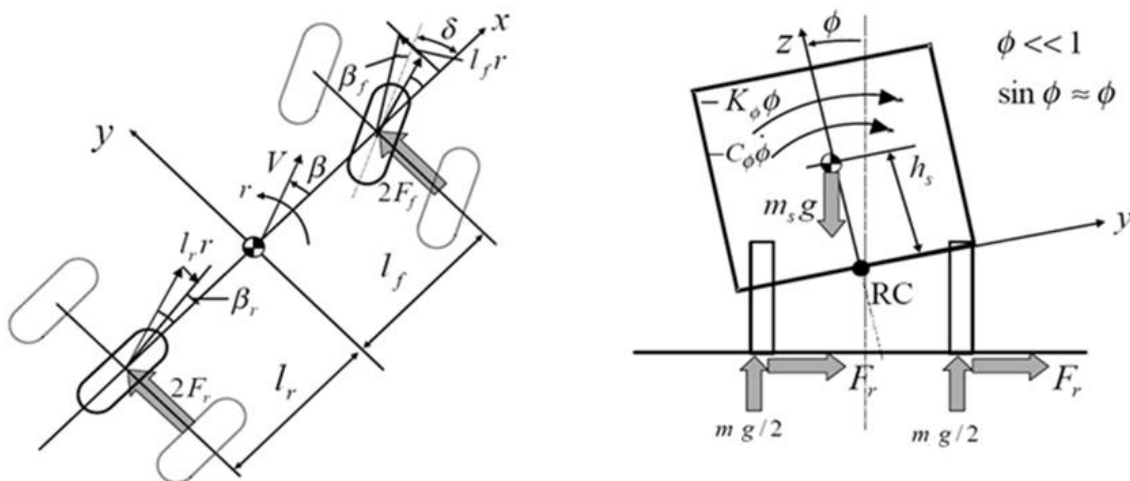


**Figure 2.8: Three DOF Automobile Model**

Lateral acceleration:

$$m\dot{V} + r = m_s h_s \ddot{\phi} - 2F_f - 2F_r \quad (2.4)$$

Yaw motion:

$$I\dot{r} + I_{xz} \ddot{\phi} = 2l_f F_f - 2l_r F_r \quad (2.5)$$

Roll motion:

$$I \ddot{\phi} + m_s h_s V \dot{\phi} + r = I_{xz} \dot{r} + M_x \quad (2.6)$$

Here,  $m$  and  $m_s$  are total vehicle mass and sprung mass, and  $I$  and  $I_\phi$  the yaw and roll moments of inertia, respectively;  $I_{xz}$  is the product of inertia with respect to the  $x$  and  $z$  directions;  $l_f$  and  $l_r$  are the distances from the center of gravity to the front and rear axle, respectively;  $F_f$  and  $F_r$  are the lateral forces produced by each of the front and rear tires, respectively;  $h_s$  is the length of the roll moment arm, which is the distance from the vehicle roll center to the center of gravity;  $M_x$  stands for the roll moment acting on the sprung mass;  $V$  is the vehicle speed and  $g$  is the gravitational acceleration. The tire forces and the roll moment are modeled as:

$$F_f = K_f \left( \delta_f + \frac{l_f r}{V} \right) \quad (2.7)$$

$$F_r = K_r \left( \delta_r + \frac{l_r r}{V} \right) \quad (2.8)$$

$$M_x = K_\phi \phi + C_\phi \dot{\phi} \quad (2.9)$$

Where  $K_f$  and  $K_r$  are the cornering stiffness of the front and rear tire, respectively (2). The steer angle of the front wheels is denoted by  $\delta$ .  $K_\phi$  is the roll stiffness and  $C_\phi$  is the roll damping coefficient.  $\alpha_f$  and  $\alpha_r$  are the roll-steer of the front and rear wheels, respectively, and can be described by the following (2):

$$\delta_f = \frac{f}{V} \quad (2.10)$$

$$\delta_r = \frac{r}{V} \quad (2.11)$$

## 2.7 Observers

Some physical variables are difficult to measure directly in real situations. Hence, an indirect method has to be applied to measure them. An observer or estimator is a mathematical entity which uses available measurements and a system model to estimate the unmeasurable variables (6). An observer is an algorithm which describes the variation of the unmeasurable from the measured inputs and outputs of the system. A schematic representation of the observer method is presented in Figure 2.9. It is almost impossible to measure side slip angle directly. Hence an observer has to be built to estimate it.

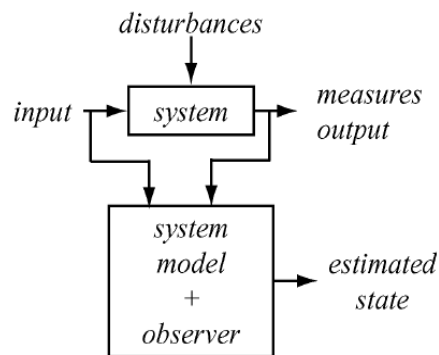


**Figure 2.9: Observer Algorithm (6)**

## 2.8 Current Approaches to Estimate Side Slip:

The side slip angle depends upon factors such as the tire orientation, direction, speed of the tire and vehicle, road-tire interface properties (especially in the non-linear region of lateral force vs. slip angle graph), tire pressure, wear, vehicle loads, braking, longitudinal slip etc. Many of these variables are difficult to sense. It is often a better idea to design observers to estimate slip angles, rather than measure them. Following are some methods to measure or estimate the side slip:

1. Researchers have looked at the idea of installing freely steered castors (7) on the front and rear axles. As the vehicle moves, the angles made by the castors with the vehicle centerline can be used to estimate tire slip angles.
2. A common technique for estimating the side slip angle is to use Inertial Sensors (4) which provide an estimate of acceleration of the vehicle. Integrating the acceleration provides velocity. This velocity estimate may be used (for example) in Equation 2.3 to estimate side slip angle if the attitude of the vehicle is known. Integrating an automotive grade accelerometer with gravity compensation gives the velocity and rate gyro gives the attitude. However, the method is limited by concerns of accelerometer/gyro measurements which get accentuated by the process of integration.
3. An improvement over inertial sensors is the use of two Global Positioning System (GPS) sensors (4) to determine vehicle velocity and attitude. GPS sensors can provide very high precision position coordinates of the sensor. Differentiating the position coordinates with time gives a good estimate of velocity. However, GPS sensors have a drawback of low update speed which makes it unsuitable for use in advanced vehicle control systems. Integrating the GPS measurements with INS values provides a good refresh rate. GPS measurements can also provide roll and pitch angles of the vehicle which can be used for analysis in more accurate non-linear dynamic modeling of vehicles.
4. Another algorithm as proposed by (5) is to estimate yaw rate using kinematic relations, either from the measured speed of the wheels or from measured lateral acceleration. Optical sensors provide angular velocity of the wheels, which are multiplied with estimates of respective wheel radii to get the wheel speeds. The difference in wheel speeds divided by the distance between the wheels gives the yaw rate. Lateral Acceleration is measured using inertial sensors. Then confidence level information is fused with each of the estimates. While braking, the confidence level of estimating yaw rate from estimated speeds of wheels goes down. Similarly, the confidence level of yaw rate estimate

using inertial sensors is high when the vehicle is in steady state, and is low when the vehicle is in a quick transient maneuver. The calculated weighted average of initial estimates is fed into an observer along with estimates of surface coefficient of adhesion to predict side slip angle

# *Chapter 3*

## ***ADAMS Model and Experimental Verification***

### *3.1 Introduction*

Vehicle models were built in ADAMS in order to analyze the mechanisms and predict the behavior under candidate test conditions. A half-car model was built for static analysis of the vehicle in which variation of lateral forces vs. steering torque for various suspension positions is studied. A full car model was built for dynamic analysis of the vehicle in which various tests have been conducted to verify the model and predict the dynamic behavior of the vehicle. On road tests were conducted on an SUV instrumented to acquire the required data.

### 3.2 Static Model

A half-car model based on Strut-McPherson suspension and rack and pinion steering mechanism was made in ADAMS (Figure 3.1) to analyze relationship between steering torque, lateral force and suspension travel. The controllable inputs to the model are steering rack displacement and height of tires. The outputs of interest include steering force and lateral force.

#### *3.2.1 Model Assumptions*

1. **Wheels:** The wheels are modeled as cylinders which can rotate about their axes which are in turn held by the suspension. The normal force between the ground and the tire is modeled as impact force acting perpendicular to the ground. As this is a static model, the lateral force has been produced using torsion springs.

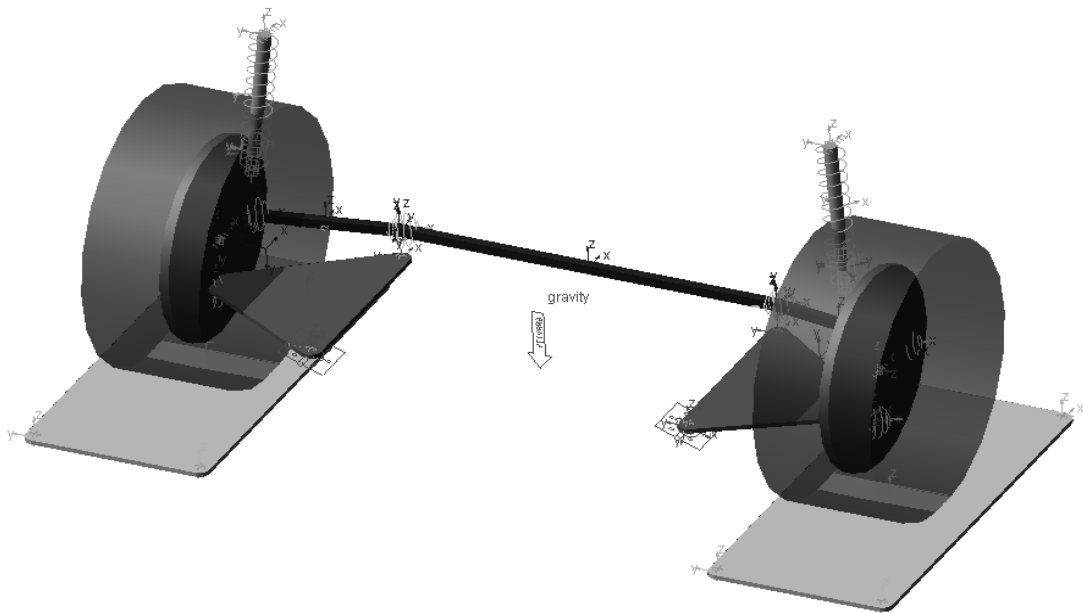


**Figure 3.1: ADAMS Static Model**

2. Suspension: The suspension has been modeled as Strut McPherson, with the tire hub attached to the A-arm with ball and socket joints. The shock absorber is attached at one end to the body and at the other to the wheel spindle with cylindrical joint.
3. Steering Mechanism: The steering mechanism is 4-bar rack and pinion type. The tie rods are connected with the rack and the wheel hub with ball and socket joints. The rack can be moved horizontally with respect to the body.

### *3.2.2 Model Predictions*

The height of the tires was changed by moving the contact patches they rest upon. Fixed steering input was given for different suspension positions and the variation of steering torque and lateral force was observed. Fig 3.2 shows sample predictions.

It is observed that for same lateral force at the tires, the Steering torque is different for different suspension positions.

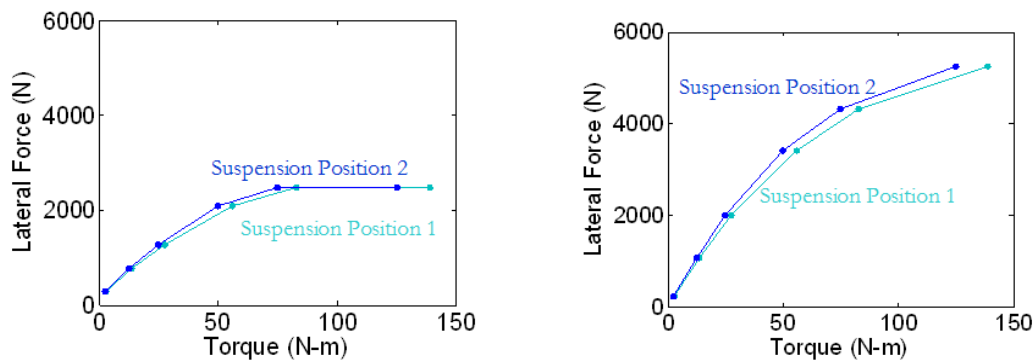


Figure 3.2: Lateral Force vs. Steering Torque (Left and Right Tires)

### 3.3 Dynamic Model

Based on the 3 Degree of Freedom model presented in 2.6.2, the vehicle was modeled in ADAMS, to analyze the dynamic behavior of the vehicle under specific test conditions. The controllable inputs in this model are vehicle velocity and steering input (rack displacement). The dynamic variables analyzed are yaw rate, lateral acceleration, roll and steering force. Figure 3.3 shows the model and each part is explained below.

#### 3.3.1 Model Assumptions

1. **Wheels:** The wheels (Figure 3.3 1-4) are modeled as cylinders which can rotate about their axes which are in turn held by the suspensions. The normal force between the ground and the tire is modeled as impact force acting perpendicular to the ground. The friction force is assumed to be linear, acting perpendicular to the normal force, in the opposite direction of the tendency of motion of the tires. The static and dynamic coefficients of friction are assumed to be 0.7 and 0.4 respectively which correspond to rubber tires on dry asphalt road.
2. **Suspensions:** The front suspension is Double-Wishbone type. The upper (Figure 3.3 5, 6) and lower (Figure 3.3 7, 8) control arms (wishbones) are attached to the body by revolute joints and the wheel hubs are mounted on the wishbones with ball and socket joints. Coil springs (Figure 3.3 9, 10) are

mounted on the dampers between the lower control arm and the body. The rear suspension (Figure 3.3 11, 12) is modeled as a long thin bar connected to the body by two vertical coil-springs and dampers. The horizontal travel of the axle due to vertical travel of the suspension is neglected.

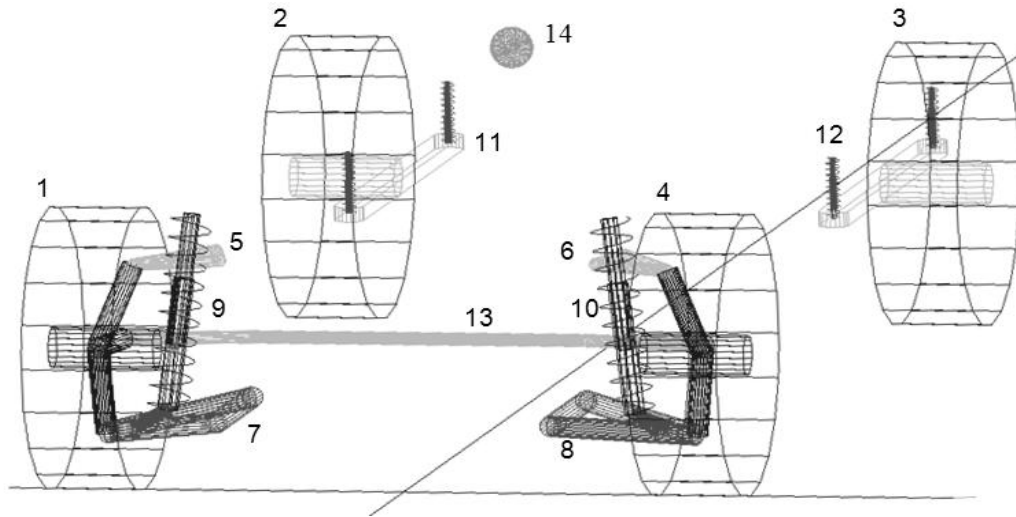


**Figure 3.3 ADAMS model of 3 DOF vehicle model**

3. **Steering Mechanism:** The steering mechanism (Figure 3.3 13) is 4-bar rack and pinion type. The tie rods are connected with the rack and the wheel hub with ball and socket joints. The rack can be moved horizontally with respect to the body.
4. **Other Assumptions:** All the sprung weight (2200 Kg) of the vehicle is concentrated at a single point (Figure 3.3 14) which is in the middle of the wheelbase (2.6m) and track (1.4m) and is at a height of 0.9 m from the ground. The unsprung weight is 275 Kg. The yaw moment of inertia is 5000 Kg-m<sup>2</sup>.

### *3.3.2 Test Conditions*

To study the predictions of the ADAMS model and to analyze the variables and parameters that influence the necessary output variables of interest, the following test

conditions are considered. The specific choice of these test conditions was motivated by what experiments could be performed on experimental vehicle.

1. Constant Radius: The vehicle is driven around a circular track of known radius with varying lateral acceleration.
2. Swept Steer: At a constant longitudinal speed, the steering input is increased until specific lateral acceleration is achieved.
3. On-Centre: In this test, the vehicle is driven at a constant longitudinal speed, and a sinusoidal steering input is given.

### *3.3.3 Model Predictions*

Figures 3.4-3.8 show the predictions of the tests carried out in ADAMS. These results are compared with the experimental results from (4) and (8). The experimental data presented in (4) and (8) corresponds to heavier vehicles; hence a qualitative comparison is carried out. For the ADAMS model, the longitudinal vehicle speed is 8 m/s. The steering input (rack displacement) for on-centre event is shown in Figure 3.4a. The corresponding steering force to be applied to maintain the steering input is shown in Figure 3.4b.

The yaw rate for this given input is shown in Figure 3.5a. The yaw rate of the ADAMS model varies in a similar manner as that of the experimental data in (4) given in Fig 3.6, but the limits of yaw rate of ADAMS model are higher due to lesser weight and smaller wheelbase. The sideslip variation of the front wheels is shown in Figure 3.5b. Slip angle variation with lateral acceleration is plotted in Figure 3.7b. The slip angles in ADAMS model in Figure 3.7a are slightly larger for similar lateral accelerations from experimental data reported in (8) which are shown in Figure 3.7b. The roll angle of the vehicle is shown in Figure 3.6a. The roll angles from the experimental values in (4) are given in Figure 3.6b. 3.8a, b give the simulated and experimental variations of steering angle with lateral acceleration.

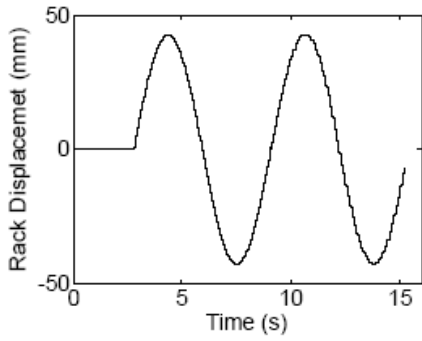


**Figure 3.4 a: Steering Input for on-center event (ADAMS Model)**

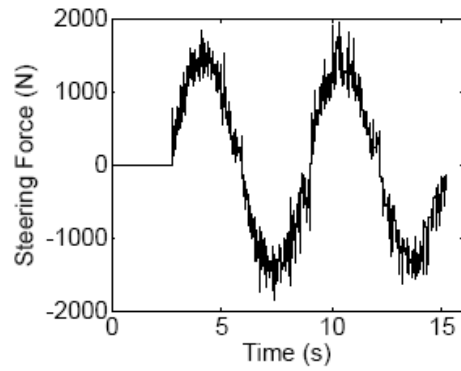


**Figure 3.4 b: Steering Force for on-center event (ADAMS Model)**

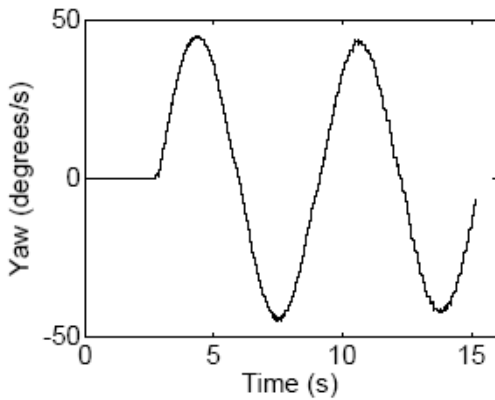


**Figure 3.5a: Yaw Rate for on-center event (ADAMS Model)**

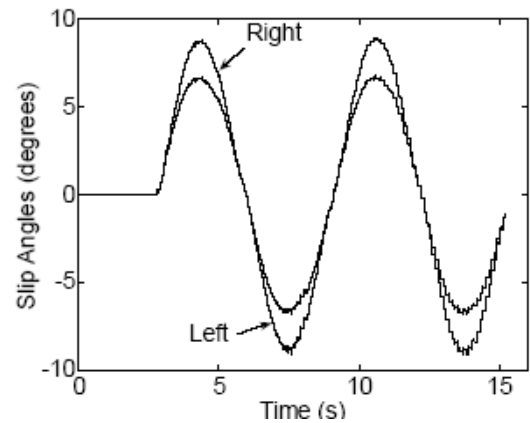


**Figure 3.5b: Front Tires' Slip Angles for on-center (ADAMS Model)**

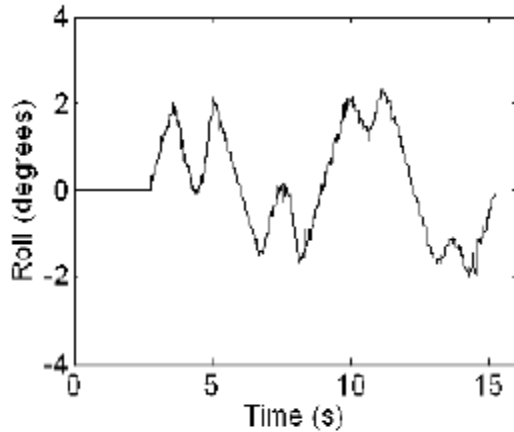


**Figure 3.6a: Roll Angle for on-center event (ADAMS Model)**

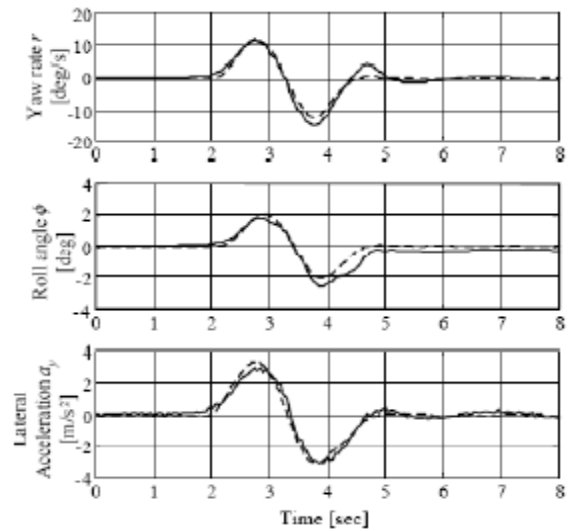


**Figure 3.6b: Experimental Values from (4)**

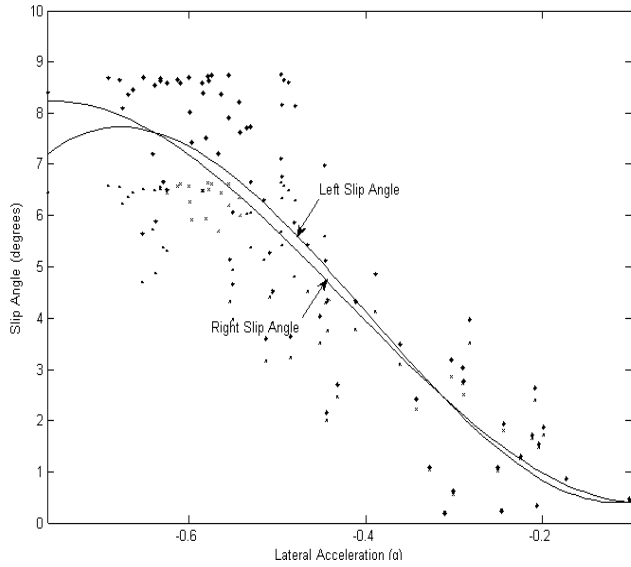


**Figure 3.7a: Slip Angle vs. Lateral Acceleration (ADAMS)**

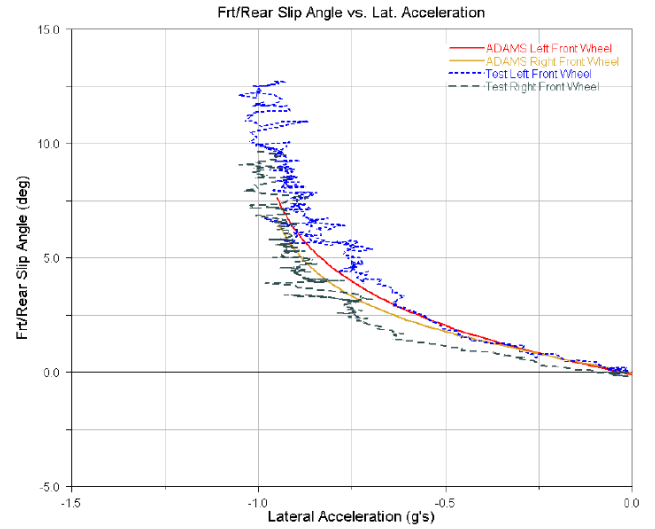


**Figure 3.7b: Experimental Values of Slip Angle vs. Lateral Acceleration from (8)**

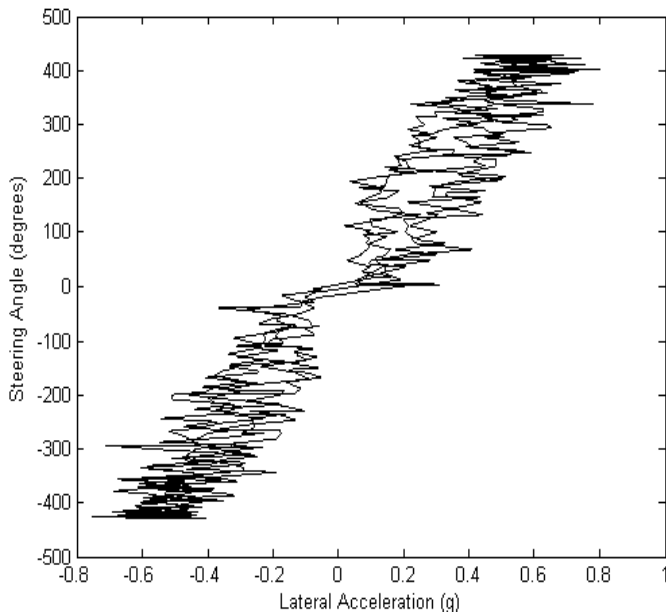


**Figure 3.8a: Steering Angle vs. Lateral Acceleration (ADAMS Model)**

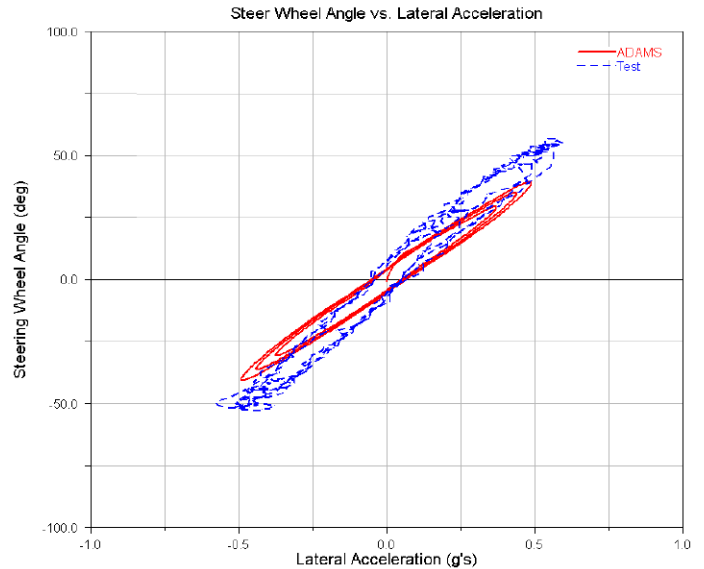


**Figure 3.8b: Experimental Values of Steering Wheel Angle vs. Lateral Acceleration (8)**

### 3.4 Experiments of Test Vehicle

This section presents the results of experiments conducted on an SUV class vehicle. The purpose of these experiments is to investigate if the ADAMS model provides reasonable estimates of side slip angle.

### *3.4.1 Data Acquisition*

From the behavior of the ADAMS model it was determined that longitudinal velocity, steering rack displacement (steering angle), torque applied to the steering wheel, suspension travel (roll of vehicle, and geometry of the steering mechanism), yaw rate and lateral acceleration were significant variables to be measured. This section gives an account of the sensor setup and techniques and devices used to gather the data from the tests conducted.

#### *3.4.1.1 Vehicle Used*

The data acquisition is set up on an SUV, Mahindra Scorpio, which has a rack and pinion type power assisted steering and a double wishbone suspension. The sprung weight of the vehicle is 2200 Kg. app. The wheelbase is 2.6m and track length is 1.4m. The unsprung weight of the vehicle is 275 Kg. The yaw moment of inertia was estimated to be 5000 Kg-m<sup>2</sup>.

#### *3.4.1.2 Hardware for Interfacing Sensors to Computer*

The sensors used for data acquisition produce analog signals which have to be suitably converted for interfacing with a digital computer. The analog signal is converted using Analog to Digital Converter chip (Texas Instruments' ADC-0809 chip). The digital signal from the ADC chip is fed to a laptop through parallel port. The laptop also controls the ADC chip. A Printed Circuit Board (PCB) has been made to mount the ADC chip along with buffers to prevent the chip and laptop being exposed to high voltages. Four analog inputs can be converted to digital signals using the current setup.

#### *3.4.1.3 Suspension Travel*

As the individual suspension on each side is a 1 DOF 4-bar mechanism, position of one link can describe the orientation of the suspension. To do this, absolute angles of the upper control arms are measured. A gear (108 teeth) is mounted and kept stationary on the point where the upper control arm is attached to the chassis (Figure

3.9). Hence the axis of the gear coincides with the axis of rotation of the upper control arm. A potentiometer is fixed on the upper control arm and a small pinion gear (12 teeth) is mounted on its axis. The pinion is made to mesh with the stationary gear mounted on the chassis. Thus, the pinion rotates when the control arm moves and the potentiometer gives an amplified measure of the angle turned by the upper control arm with respect to the chassis. The analog input is fed to the laptop using the ADC setup described earlier.

#### *3.4.1.4 Steering Torque and Angle*

The steering torque and angle are measured using a Strain-Gage principle Torque Transducer Sensor which gives analog signals for angle and torque. As the signals produced by the strain gauges are very low to be analyzed by the ADC 0809 chip, they are amplified using San-ei N9224 amplifier. The amplified analog signal is then converted to digital signal using the ADC setup described earlier.

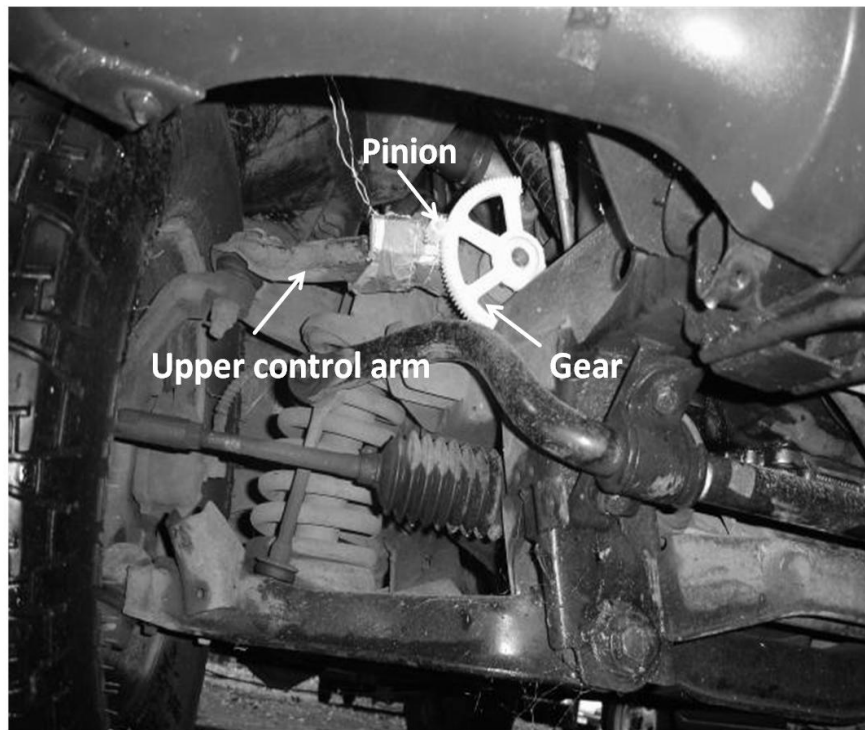


**Figure 3.9: Arrangement of gears and potentiometer for measuring suspension travel**

### *3.4.1.5 Yaw Rate and Lateral Acceleration*

The vehicle is driven at known speeds, on a pre marked course. Hence, by knowing the trajectory of the curve and speed of the vehicle, the yaw rate and lateral acceleration is calculated.

### *3.4.2 Summary of Estimation Methodology*

The ADAMS model is used to simulate candidate test conditions and predict the side slip angles for the tests to be conducted on the SUV. The predictions of this model have been verified with experimental results from literature. An open-loop estimator that uses a three degree-of-freedom vehicle model (equations 2.4-2.9) is used to estimate side slip angles from the measured and assumed experimental data from tests conducted on the SUV. The test conditions and results are explained below.

### *3.4.3 Vehicle Tests*

#### *3.4.3.1 Constant Speed around Circle of Fixed Radius*

The vehicle longitudinal velocity was maintained at 20kmph while moving along a circle of radius 11m. Figure 3.10 gives the data acquired from the test the calculated slip using equations 2.4-2.9.

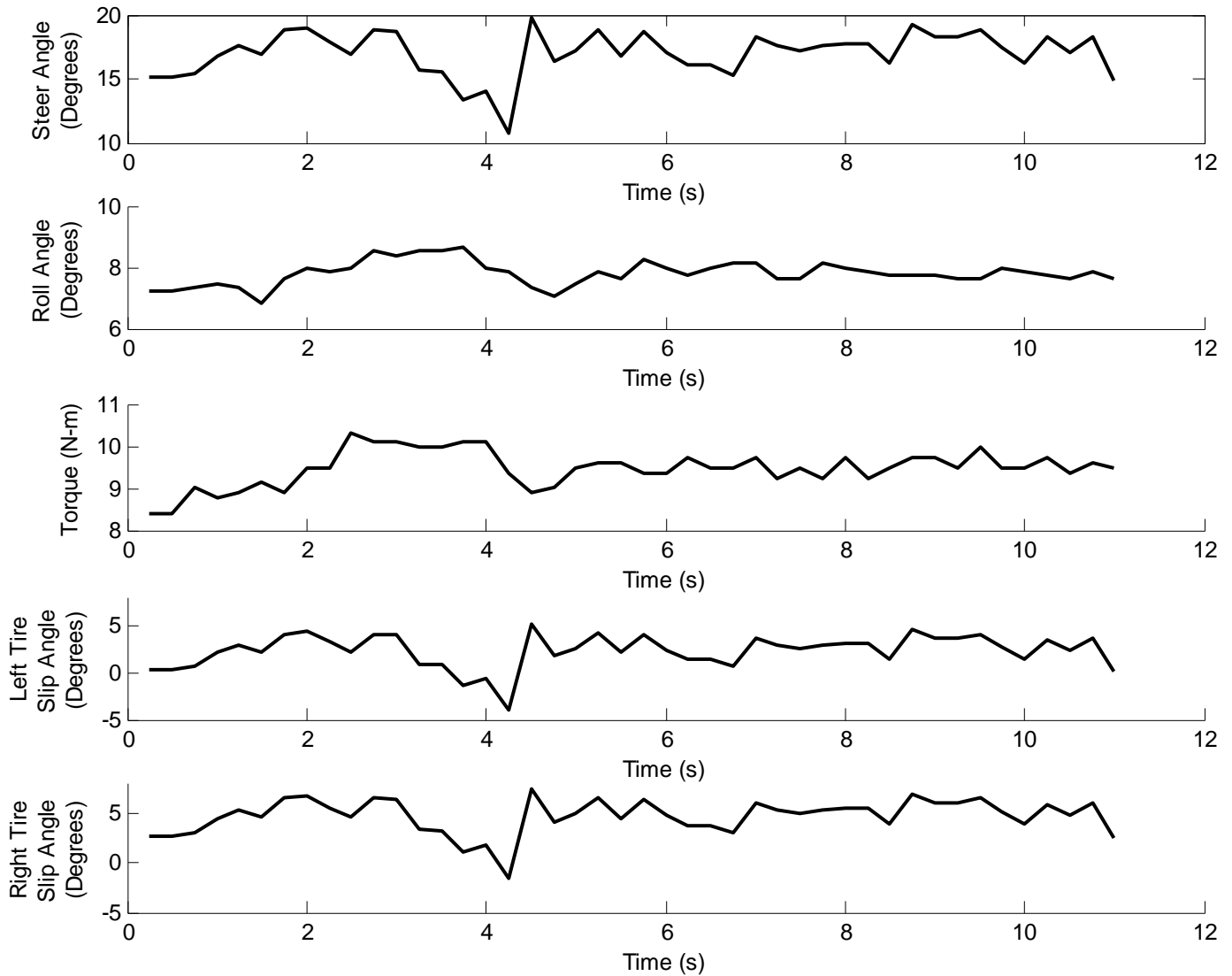


**Figure 3.10: Experimental data and Side Slip Angle Estimates for Longitudinal Speed 20 kmph around 11m radius curve**

### 3.4.3.2 Decreasing Speed around Circle of Fixed Radius

The vehicle was accelerated to 20kmph and then decelerated slowly to 10kmph while moving along a circle of radius 11m. After some time the vehicle was brought to rest, all the while moving along the circle of radius 11m. Figure 3.11 gives the data acquired from the test and the estimation of side slip angles using equations 2.4-2.9.

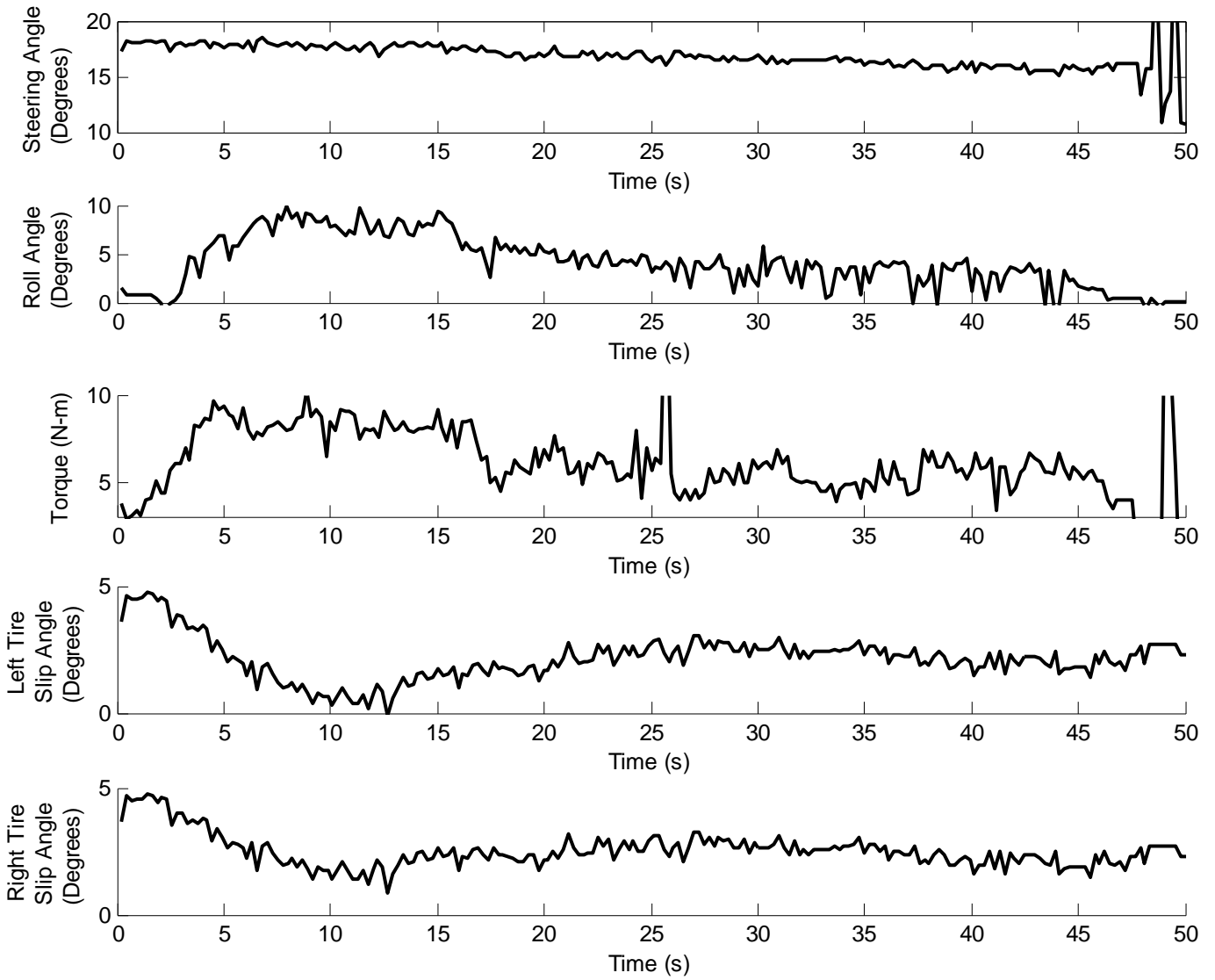


**Figure 3.11: Experimental data and Side Slip Angle Estimates for Decreasing Longitudinal Speed around 11m radius curve**

The side slip angle predictions of the ADAMS model for these test conditions are given in the Figure 3.12:

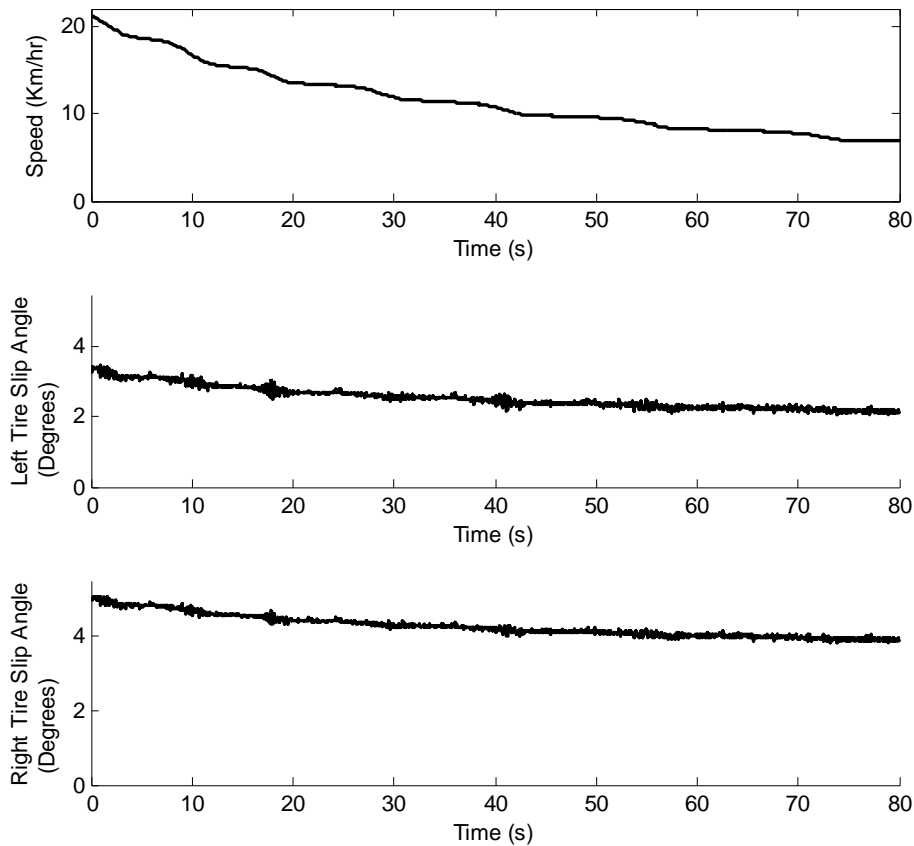


**Figure 3.12: Side Slip Angle Estimates from ADAMS model**

### *3.5 Observations*

The analysis of data acquired in tests explained in 3.4.3, and using the estimation scheme described in 2.6.2, the results are:

1. The side slip angle of the front right tire is estimated to be around 4.7 degrees for a longitudinal speed of 20 km/hr of the SUV around a circle of radius 11 meters.
2. The side slip angle of the front left tire is estimated to be around 3.3 degrees for a longitudinal speed of 20 km/hr of the SUV around a circle of radius 11 meters.

3. The side slip angle of the front right tire is estimated to be around 2.8 degrees for a longitudinal speed of 10 km/hr of the SUV around a circle of radius 11 meters.
4. The side slip angle of the front left tire is estimated to be around 2.6 degrees for a longitudinal speed of 10 km/hr of the SUV around a circle of radius 11 meters.

### *3.6 Discussion*

The open-loop estimates of side slip based on the 3 Degree of Freedom model (equations 2.4-2.9) match well with the predictions of the ADAMS model. For speed of 20kmph the slip values are in the range 4-5 degrees. However, the slip angle estimates decrease more than expected when the vehicle decelerates. Again when the vehicle moves at constant speed, the slip angle estimates match well with the theoretical predictions.

The error in estimation of the side slip angle while decelerating happens because while decelerating, tires experience extra longitudinal forces, which result in longitudinal twisting of the tire treads. Thus, the linear cornering stiffness curve (Fig2.5) assumption used in the three Degree-of-Freedom model formulation may be invalid under longitudinal acceleration.

# *Chapter 4*

## ***Conclusions and Future Work***

### *4.1 Conclusion*

This project aimed at estimating side slip angle in front-wheel steered, rear-wheel driven four wheeled vehicles. Side slip angle cannot be measured directly; hence an estimator has been built to calculate side slip angle from measurable variables. A model was constructed in ADAMS to predict this variable for a candidate set of test conditions. The SUV was instrumented to measure right and left suspension travels, steering angle and steering torque, and tests were conducted. Using the measured and assumed variables for these tests, side slip angles for tires were estimated using an open-loop estimator that is based on a three degree-of-freedom vehicle model. These estimates of side slip angle matched with the predictions of the ADAMS model for these set of conditions. Since the predictions of the ADAMS model were found to be in reasonable agreement with the experimental results reported in literature, we conclude that the three degree-of-freedom model provides good prediction capabilities for estimation of side slip angle

### *4.2 Future Work:*

We suggest the following to improve upon this work:

1. More variables like vehicle longitudinal and lateral speeds and yaw rate can be acquired for a better estimation of side slip.
2. The estimator can be made to take into account longitudinal acceleration of the vehicle.
3. More tests like lane change maneuver, on-centre test, braking in turn etc. can be conducted.
4. Conditions like tire pressure, load, load distribution etc. can be varied to check their affect on the vehicle response.

# References

1. **Gillespie, T. D.** . *Fundamentals of Vehicle Dynamics*. Warrendale, PA : Society of Automotive Engineers, Inc., 1992
2. *www.sae.org*.
3. **Pacejka, H.B.** . *Tyre and Vehicle Dynamics*. s.l. : Butterworth-Heinemann, 2002
4. Integrating Inertial Sensors with GPS for Vehicle Dynamics Control. **Gerdes, J C and Ryu, J.** . , 2004, Journal of Dynamic Systems, Measurement, and Control
5. Estimation of Vehicle Side Slip Angle and Yaw Rate. **Hac, A., Simpson M.D.** . , 2000-01-0696, SAE Technical Paper
6. Virtual Sensor: Application to Vehicle Sideslip Angle and Transversal Forces. **Stéphane, J., Charara, A., Meizel, D.** . , 2004, IEEE transactions on Industrial electronics, Vol. 51, No. 2, 278-289
7. Closed-loop Design for Decoupling Control of a Four-wheel Steering Vehicle. **Yeh, E.C., Wu, R.H.** . , 1989, International Journal of Vehicle Design, Vols. 10, no. 6, 703-727
8. Study on a vehicle dynamics model for improving roll stability. **Takano, S., Nagai, M, Taniguchi, T, Hatano, T.** . , 2003, JSAE Review 24, 149-156
9. Developing an ADAMS Model of an Automobile Using Test Data. **Rao, P.S., Roccaforte, D., Campbell, R., Zhou, H.** . s.l. : SAE Technical Paper 2002-01-1567, 2002
10. A study on lateral speed estimation methods. **Ungoren, A.Y., Peng, H. and Tseng, H.E.** . , 2004, Int. J. Vehicle Autonomous Systems, Vol. 2, Nos. 1/2, 126-144
11. Slip Angle Estimation for Vehicles on Automated Highways. **Saraf, S., Tomizuka, M.** . , 1997, Proceedings of the American Control Conference 0-7803-3832-4/971, 1588-1592
12. Nonlinear State and Tire Force Estimation for Advanced Vehicle Control. **Ray, L.R.** . , 1995, IEEE transactions on control systems technology Vol. 3, No 1, 117-124
13. Optimal yaw moment control law for improved vehicle handling. **Esmailzadeh, E., Goodarzi, A., Vossoughi, G.R.** . , 2003, Mechatronics 13, 659-675

